

<https://doi.org/10.1038/s44271-025-00224-7>

Recent, but not long-term, priors induce behavioral oscillations in peri-saccadic vision

Check for updates

Xin-Yu Xie ¹✉, David C. Burr^{2,3} & Maria Concetta Morrone ⁴

Perception of a continuous world relies on our ability to integrate discontinuous sensory signals when we make saccadic eye movements, which abruptly change the retinal image. Here we investigate the role of oscillations in integrating pre-saccadic information with the current sensory signals. We presented to participants ($N = 24$) a brief pre-saccadic Gabor stimulus (termed the *inducer*) before voluntary 16° saccades, followed by a *test* Gabor stimulus at various times before or after saccadic onset. Orientation judgments of the test stimulus were biased towards the orientation of both the inducer and previous (1-back) test stimulus, consistent with serial dependence. In addition to the average bias, judgments oscillated in synchrony with saccadic onset at alpha frequencies (~ 9.5 Hz) towards the orientation of the inducer or 1-back stimulus. There was also a strong bias towards the mean orientation (central tendency): however, that bias was constant over time, not associated with saccade-synched oscillations. Perceptual oscillations in serial dependence (but not central tendency) suggest that alpha rhythms may be instrumental in communicating short-term (but not long-term) perceptual memory across saccades, helping to preserve stability during saccades. The distinction between the modes of communicating short- and long-term memory suggests that the two phenomena are mediated by distinct neuronal circuitry.

Perception is a dynamic process that relies on the integration of sensory signals, over space and over time, to construct a coherent representation of the surrounding world. One of the key challenges is understanding how the brain maintains a sense of perceptual continuity from discontinuous sensory input, particularly during saccadic eye movements. Saccades are rapid, ballistic eye movements, which occur many times per second, posing significant challenges to the perception of a stable and continuous visual world. Many studies have found that perception is strongly suppressed and distorted during saccades (for review, see refs. 1,2). But most of the time perception remains stable, despite the radical saccade-induced changes to the retinal images.

It has been suggested that *continuity fields* – spatiotemporal integration mechanisms that continuously bias perception and cognition towards previously encountered information promote the stability by smoothing perceptual representations³. Strong evidence for the existence of continuity fields comes from the recently described phenomenon of *serial dependence*^{4,5}, where the perception of the current stimulus is biased towards previous stimuli in a sequence. Serial dependence occurs both for simple

visual features, such as orientation or color, as well as for complex features, such as face identity and gender, beauty, body weight and quality of art (for reviews see ref. 6–8). Studies suggest that the bias induced by serial dependence is not a system flaw but rather leads to more efficient perception^{5,9} (but see also refs. 10–12).

Perception is affected not only by recent past stimuli, but also by longer-term perceptual history. Perceptual estimates of almost every quantity, including size, time, and number, gravitate toward the average of the response space, a phenomenon known as *regression to the mean*, or *central tendency*¹³. *Regression to the mean* is well described within the Bayesian framework, where the mean, computed over several trials, is considered the *prior*, which combines with sensory data (the *likelihood*), following Bayes's rule. The use of the mean as a prior has also been shown to be an efficient strategy, reducing estimation error^{14,15}, as happens with serial dependence. Under normal experimental conditions, the two types of history-based expectations interact, together with other phenomena such as adaptation^{16,17}.

Experimental studies of temporal contextual effects typically involve artificially altering stimuli between trials, within an otherwise static

¹School of Psychology and Cognitive Science, East China Normal University, Shanghai, China. ²Department of Neuroscience, Psychology, Pharmacology, and Child Health, University of Florence, Florence, Italy. ³School of Psychology, University of Sydney, Camperdown, NSW, Australia. ⁴Department of Translational Research on New Technologies in Medicine and Surgery, University of Pisa, Pisa, Italy. ✉e-mail: xyxie@psy.ecnu.edu.cn

environment. However, a natural testbed for studying integration of spatio-temporal information in successive stimuli is during saccadic eye-movements, which change the retinal input of stable scenes. To preserve stable visual continuity, the input of successive fixations before and after each saccade needs to be integrated. Many processes are at work, including suppression^{18–21}, “remapping”^{22,23}, and other more complicated phenomena². Most of these phenomena show a strong predictive component: the visual mechanisms are predictively alerted to the future stimulus it will be sensing^{23,24}. Trans-saccadic integration has been well described in Bayesian terms, as an optimal integration process^{25,26}, taking into account the inherent uncertainty of vision at the time of saccades. Much evidence is consistent with the idea that trans-saccadic integration is instrumental in maintaining perceptual continuity²⁷. Contextual effects, such as serial dependence, are strongest at saccadic onset²⁸.

A good deal of evidence has accumulated to suggest that neural oscillations in the alpha and low-beta range are implicated in serial dependence, and predictive perception in general. Theoretical arguments suggest that generative feedback could create neural oscillatory reverberations in the alpha range^{29–31}. The idea is that perceptual oscillations – particularly in bias – could result from the predictive feedback loop involved in updating of expectations. This idea has received firm experimental support. Ho et al.³² showed that alpha-frequency oscillations in auditory judgments occurred only when the previous stimulus was presented to the same ear as the current one. Similarly, judgments of the gender of faces showed strong oscillations in the low-beta frequency, dependent on the gender of the previous face: 14 Hz if the previous face was female, 17 Hz if it was male³³.

Evidence also points to the role of neural oscillations, particularly at alpha frequencies, in the maintenance of working memory. For example, Jensen et al.³⁴ reported significant EEG responses in the 9–12 Hz range during the retention interval of working memory tasks. Similarly, Wianda and Ross³⁵ reported alpha oscillations in MEG associated with working memory retention. VanRullen and Macdonald³⁶ claimed that “perceptual echoes” near 10 Hz reflect brain mechanisms for retaining and processing short-term prior information. While some theories suggest that alpha-band activity reflects the active inhibition of task-irrelevant information^{37,38}, these oscillations appear crucial for the temporary storage, temporal ordering, and manipulation of sensory inputs within working memory^{39–41}. By inhibiting task-irrelevant brain regions, alpha oscillations ensure that relevant stimuli are maintained in an accessible state for subsequent processing and decision-making. These findings support the notion that oscillatory activity is integral to the dynamic updating and utilization of prior experiences in working memory.

Oscillations are also strongly linked to saccadic (and other) movements⁴². Neurophysiological work shows that in area V4 of the monkey, alpha oscillations become coherent between sites active before and after saccades, suggesting they serve an active role in maintaining trans-saccadic continuity⁴³. Psychophysical results also point to a major role of alpha rhythms during saccades. For example, bias of orientation oscillates synchronized to the saccade onset at alpha rhythms⁴⁴, while sensitivity oscillates at low theta or delta frequencies^{45,46}. There is also EEG and MEG evidence that saccades synchronize neuronal endogenous rhythms^{47,48}, and that the power of these oscillations is modulated by the specific trans-saccadic task⁴⁹. Thus there is good reason to suspect that alpha rhythms could be involved in perceptual expectations at the time of saccades. We therefore examined the role of oscillations in perceptual prediction at the time of saccades, using a serial-dependence paradigm.

Methods

We ran two separate experiments, one where participants made horizontal saccades from left to right, the other vertical saccades from top to bottom. Some preliminary data on horizontal saccade average serial dependence has already been published²⁸. There was no preregistration of this study.

Participants

Twelve participants participated in the horizontal saccade experiment (6 Women, 6 Men; Age: 26.9 ± 3.0) and twelve different participants took

part in the vertical saccade experiment (5 Women, 7 Men; Age: 23.6 ± 4.0). Gender and age were self-reported. All had normal or corrected-to-normal vision and provided written informed consent before taking part in the study. With the exception of one author (XIE), all were naive to the purpose of the experiment. Experimental procedures were approved by the regional ethics committee (Comitato Etico Pediatrico Regionale—Azienda Ospedaliero-Universitaria Meyer—Firenze, FI). Participants were not paid for their time.

Apparatus

Experimental measures were performed in a quiet and dimly lit room. Stimuli were generated with Psychtoolbox 3 in MATLAB r2020b (The MathWorks), and presented with PROPixx projector (VPixx Technologies Inc., Canada) by back projection onto a screen (Epson ELP-SC21B, 180 × 100 cm) with a resolution of 1920 × 1080 pixels and a refresh rate of 120 Hz. Participants sat 1 m from the screen, which subtended 90 × 50 cm. Head position was stabilized by a chin and headrest. Experiments were run in a dark room. The position of one eye was monitored at 1000 Hz with the EyeLink 1000 system (SR Research, Canada). Nine-point calibration and validation was made at the beginning of each session, and eye drift corrected at the beginning of each block.

Stimuli and procedures

The *test* and *inducer* stimuli were Gabor patches (Gaussian-windowed sinusoidal gratings) presented at the center of a uniformly illuminated screen background (mean luminance 135 cd/m²). The Gabor stimulus was 3 cycle/deg spatial frequency, 80% contrast, 1.36° standard deviation, and random phase on every presentation (Fig. 1a).

Trials started with participants viewing a small (0.2° in diameter) fixation dot (F0), 8° left of (or above) screen center. The pre-saccadic inducer stimulus was briefly presented for 17 ms (2 monitor frames). After an 800–1200 ms random interval, F0 disappeared and a saccadic target (F1) appeared immediately 8° right of (or below) screen center. Participants saccaded directly to F1. After a random delay (10–400 ms) from the saccadic target, the *test* stimulus, a brief 17-ms Gabor patch was displayed in the center of the screen (Fig. 1a), equidistant from the two fixation points. We did not present the stimulus before the saccadic target to avoid generating a stimulus-driven saccade. Participants reproduced the test orientation by rotating the response bar by mouse. If participants did not see the test at all, they could skip the trial without responding. To ensure that participants did not completely ignore the inducer stimulus, they were required to report the approximate orientation (left or rightward tilt) of the inducer stimulus by pressing the left or right arrow at the end of 10% trials.

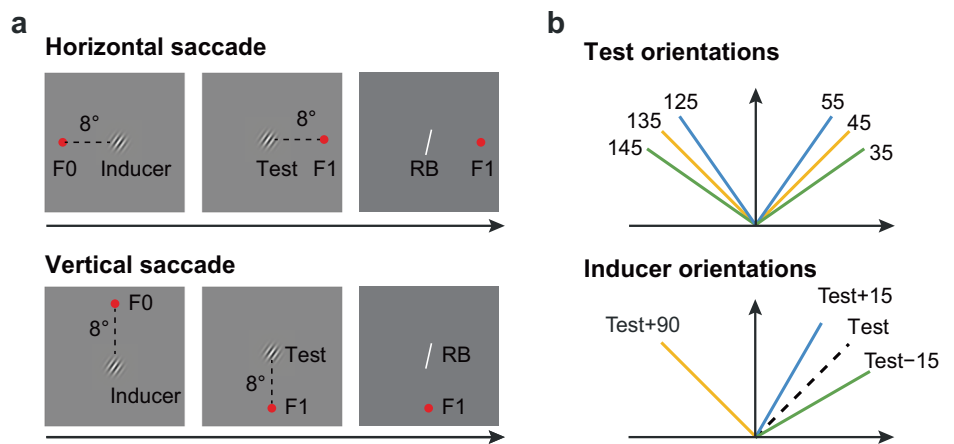
For each block, there were 60 trials in total. Six test orientations (35°, 45°, 55°, 125°, 135°, 145°) were randomly assigned in each trial (10 trials for each orientation), and the inducer orientation was randomly chosen from the positive (Test+15°), negative (Test–15°), and orthogonal (Test+90°) conditions (Fig. 1b). Each participant performed 15–20 blocks.

Data analysis

Saccade and psychophysical analysis. To analyze the saccade data, we utilized the EyeLink parsing algorithms. Saccades were distinguished from fixations based on specific thresholds: the saccadic velocity threshold was set at 35°/s, the saccadic acceleration threshold was set at 9500°/s², and the saccadic motion threshold was set at 0.15°. We excluded saccades with an amplitude smaller than 1 degree to eliminate the effects of micro-saccades.

Before analyzing reproduced orientation errors, we discarded the no-response trials and the trials in which the orientation reproduction error exceeded two standard deviations of the mean (i.e., 37.7°). A total of 11.9% and 8.8% of trials were discarded in horizontal and vertical saccade experiments, leaving on average 962 (SD = 97) and 844 (SD = 71) valid trials for each participant in both experiments (see ref. 28). The saccadic latency was 157 ms (SD = 38 ms) for horizontal saccades and 160 ms (SD = 39 ms) for vertical saccades. The standard deviation of orientation reproduction

Fig. 1 | Experimental procedures. **a** Stimulus arrangement. Participants first fixated F0, then the inducer stimulus was presented at screen center. After a random interval between 0.8 and 1 s, F0 disappeared and F1 appeared. Participants saccaded from F0 to F1 with a single saccade, as the test stimulus was presented in the center of the screen before or after the saccade onset. Participants moved the response bar (RB) to reproduce the orientation of the test stimulus. The test stimulus comprised 6 orientations, the inducer stimulus had three orientations relative to the test stimulus ($\pm 15^\circ$ or 90°).



error for the valid trials was 10.2° , compared to 18.8° for all trials. We also conducted an analysis that retained all trials, which yielded results consistent with those presented in the main text: both the inducer and 1-back stimuli elicited strong alpha oscillations of bias.

We separately calculated the orientation bias towards inducer, and towards 1-back stimuli for both horizontal and vertical saccades, scoring them as positive if towards the inducer stimulus (and negative if away), and similarly with respect to the 1-back stimulus. For each trial we calculated the delay of the test appearance from saccadic onset. The frequency analysis, and all statistical tests were performed applying a General Linear Model (below), restricting the range of delay of test from saccadic onset between -200 to 200 ms. To illustrate the time course of the errors, we applied a moving average smoothing method by fixing the number of trials; the width of the smoothing window varied from 180 to 800 trials for the various figures depending on the total number of trials. We sorted all trials from all participants by time and calculated the average orientation error and the average time within a specific smoothing trial window. The window was then moved forward, recalculating these averages. This smoothing approach helped visualize the trend (plots in Figs. 2b, 3b, 4a, 4c, 4e, 5b, 6a, and 6c). However, all statistics were performed on single, unsmoothed and unbinned trials. Standard errors of the mean were calculated by bootstrap (1000 iterations, with replacement), as the standard deviation of the bootstrap distributions for each smoothed value.

General linear model (GLM). To examine the data for oscillations and evaluate their coherence across participants, we used an approach based on single trials^{50,51}. The response bias in orientation (degrees) y_i ($i = 1, 2, \dots, n$, where n is the total number of trials) at time t_i (i.e., the times from saccadic onset to test stimulus onset in seconds) is modeled by the linear combination of sinusoidal functions at each tested frequency (f) as follows:

$$\hat{y}_i = \beta_0 + \beta_1 \sin(2\pi f t_i) + \beta_2 \cos(2\pi f t_i) \quad (1)$$

where \hat{y}_i is the predicted response and β_0 , β_1 , and β_2 are fixed-effect regression parameters estimated by standard least square method.

The regression was performed for each frequency in the range from 5 to 25 Hz with 0.1 Hz steps. For the evaluation of the average responses (amplitude and phases) across temporal frequencies, we randomly selected trials (with replacement) 2000 times and estimated β_1 , and β_2 to create a bootstrap distribution of amplitudes and phases, then vector averaged for every frequency tested (red curves in Figs. 2c, 3c, 4b, 4d, 4f, 5c, 6b, and 6d).

The significance of the model fitted in Eq. 1 was evaluated with a permutation test: we shuffled the response (orientation bias) of each individual's trials to create 2000 surrogate datasets of all aggregate data across participants and regressed each dataset with the model described in Eq. 1.

Shuffling the response and not the time is the appropriate approach keeping unchanged the numerosity of trials across time. Statistical significance was determined by calculating p -values, which represent the percentage of bootstrap amplitudes higher than the original data's amplitudes at each frequency. These p -values were subsequently corrected for multiple comparison across frequencies using false discovery rate (FDR) procedure.

To ensure that the effects were not driven by only a few participants, the frequency with maximum and significant amplitude was evaluated in the data set of each individual participant. Errors of the mean amplitude and mean phase were evaluated using 2D propagation of error, assuming a normal 2D distribution of the individual vectors around the mean. Significance was assessed by applying tests for circularity of the phase values and the Hotelling's T^2 Test.

To further validate that there were no differences in the fitted results across different saccadic directions or testing orientations, we defined the time points of peaks and troughs based on the frequency with maximum amplitude. We centered a 25-ms time window (about a quarter of a cycle at the frequency of interest) around each peak and trough, and calculated the average bias across all trials within peaks- and troughs- window for each participant, respectively. Two-way repeated measures ANOVAs were used to measure the statistical significance of amplitude (bias in peaks and troughs) and saccadic direction or test orientation. Data distribution was assumed to be normal, but not formally tested.

Reporting summary

Further information on research design is available in the Nature Portfolio Reporting Summary linked to this article.

Results

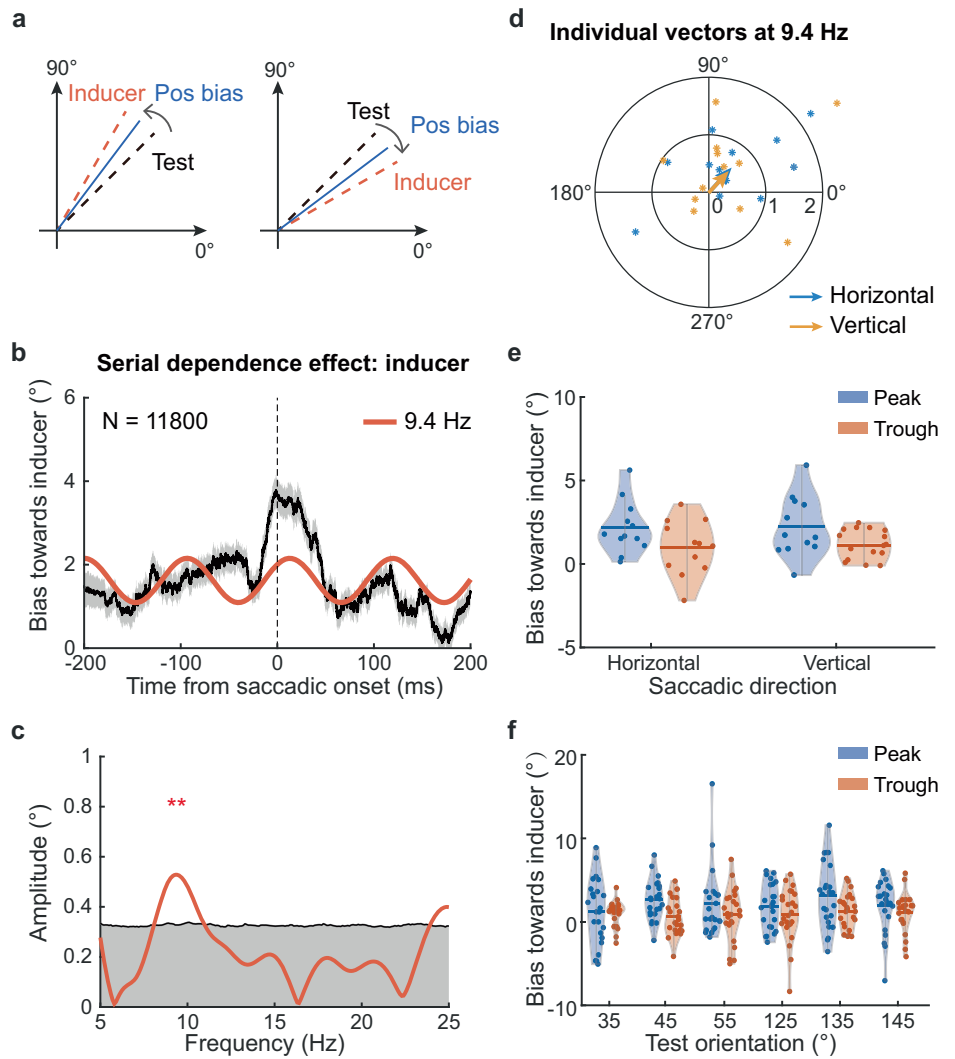
Effect of inducer

Participants made 16° horizontal (left-right) or vertical (up-down) saccades, after passively viewing an *inducer* stimulus (an oriented grating patch) presented from 1 to 2 s before saccadic onset. Their task was to reproduce the orientation of a small, brief test grating patch, presented at variable times before or after the saccadic onset (Fig. 1). The briefly presented inducer biased the reproduction of the test towards its orientation. The average bias towards the inducer was similar for Horizontal ($1.71 \pm 0.27^\circ$, $t(11) = 6.37$, $p < 0.001$, Cohen's $d = 1.84$, 95% CI [1.12, 2.30], one-sample t -test comparing with 0) and Vertical saccades ($1.40 \pm 0.29^\circ$, $t(11) = 4.74$, $p < 0.001$, Cohen's $d = 1.37$, 95% CI [0.75, 2.05]).

We next examined the dynamics of this phenomenon by measuring response bias as a function of time from saccadic onset. For this analysis, we considered only trials where the inducer was $\pm 15^\circ$ from the test, excluding the other third of trials where it was orthogonal (as they cannot be scored, Fig. 2a). This left two-thirds of the trials, 11800 in total (for both horizontal and vertical saccades). Figure 2b shows the results as a function of time from

Fig. 2 | Oscillations in bias towards inducer.

a Illustration of how responses were coded, positive if towards the *inducer*. **b** The black line shows the time course of the bias of the aggregate data, smoothed over 800 trials (for display purposes only). The gray area around the line represents ± 1 SE computed by bootstrap resampling (1000 reiterations). The colored curve shows a 9.4 Hz oscillation corresponding to the peak spectral amplitude of the combined horizontal and vertical data. **c** GLM spectral analysis of the aggregate data, where each trial bias contributed at the exact delay from the saccadic onset. The amplitude spectrum shows a clear peak around 9.4 Hz. The gray region shows the 95% confidence limits of the permutation analysis of the bias, keeping trial saccadic onset delay unaltered. ** indicates FDR corrected $p < 0.05$ in the range 5–25 Hz. **d** 2D vectors of the peak sinusoidal wave at 9.4 Hz for each individual participant for horizontal (blue dots) and vertical (yellow dots) saccades. The blue and yellow arrows show the mean vector of horizontal and vertical saccades, respectively. The length and direction of the arrows indicate the amplitude and phase (relative to time of saccadic onset). **e** The average bias from trials within a 25-ms time window around the peaks and troughs of a 9.4 Hz sinusoidal wave for horizontal and vertical saccades across subjects. **f** The average bias from trials within a 25-ms time window around the peaks and troughs of the 9.4 Hz sinusoid for each test orientation. In (e, f), the horizontal line within each violin represents the mean bias, and individual data points are overlaid as dots.



saccadic onset for all trials of all participants, for both horizontal and vertical saccades. For display purposes only, the data have been smoothed with a running window. All data fall above zero (average $1.56 \pm 0.20^\circ$), consistent with the attraction towards the inducer. However, superimposed on the average bias is a clear modulation. Spectral analysis (on single trials, using a GLM approach: Fig. 2c) shows a clear, unique and significant peak at 9.4 Hz (FDR corrected $p = 0.038$), with no evidence of other significant perceptual oscillations in the frequency range 5–25 Hz. This sinusoidal component is plotted in Fig. 2b (red trace), at appropriate amplitude and phase. Note that the sinusoid incorporates the peak in bias near saccadic onset, which is embedded within this best-frequency oscillation. The peak in serial dependence at saccadic onset is well predicted from the increased uncertainty at that time²⁸: here we further show that it is in phase with the ongoing oscillation.

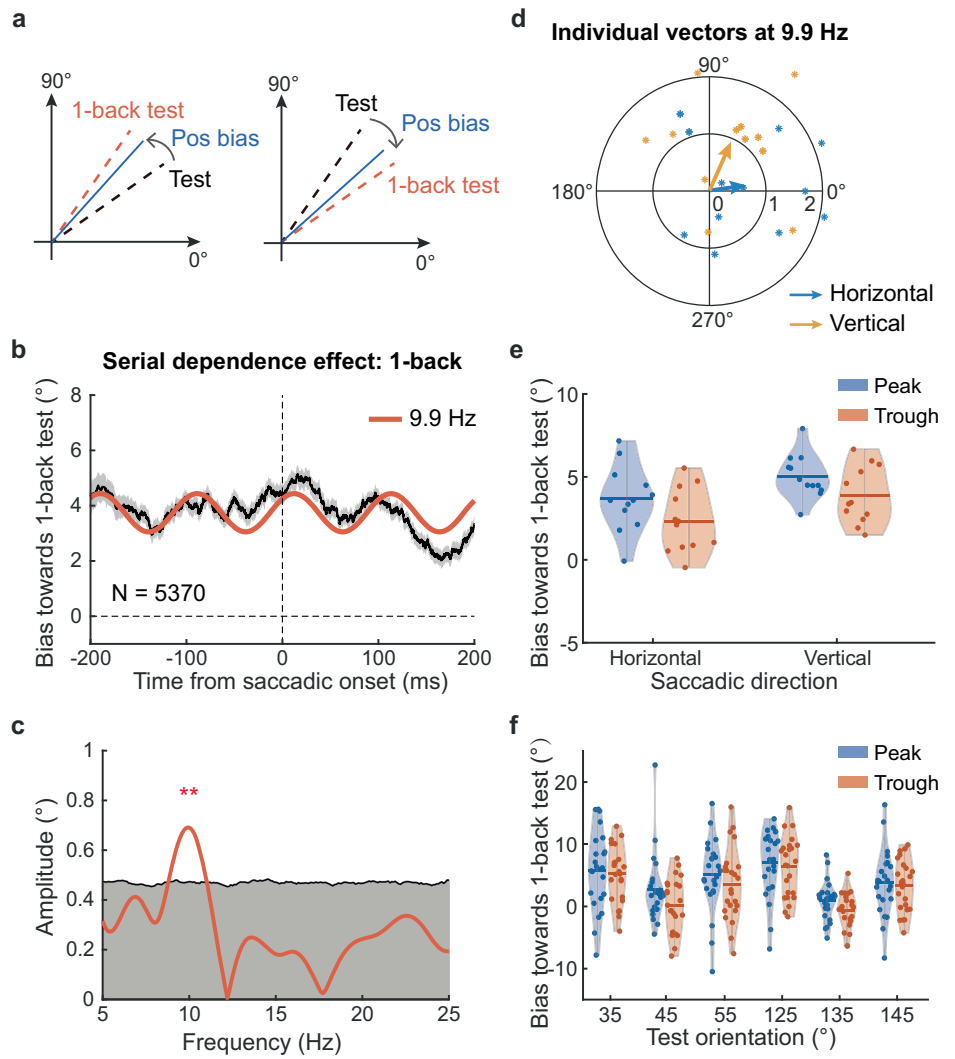
This and other major analyses of this study analyzed single trial data without binning, using a general linear model approach. This has been shown to yield the highest discriminability of real oscillations, and immune to the spurious frequencies introduced by binning^{32,51,52}. However, we also performed a more standard Discrete Fourier Transform analysis⁵² on individual participants' data (see Supplementary Materials), which similarly revealed a significant oscillation around 9.5 Hz (Mean power = 1.84 at 9.5 Hz, 95% CI = [0.92, 2.98], FDR corrected $p = 0.049$, Fig. S1).

Figure 2d is a polar plot of the amplitudes and phases at the peak 9.4 Hz sinusoidal frequency for all individual participants, separately for horizontal (blue dots) and vertical (yellow dots) saccades. The phase clustering is

significant ($47.1^\circ \pm 30.0^\circ$; Hotelling's T^2 test at 9.4 Hz: $F(2,22) = 5.51$, $p = 0.011$, $\eta^2 = 0.33$; abscissa mean = 0.41, 95% CIs [0.14, 0.68]); ordinate mean = 0.38, 95% CIs [0.03, 0.73]). The two saccadic directions yielded similar results ($47.3^\circ \pm 28.2^\circ$ for horizontal saccades, $46.9^\circ \pm 32.3^\circ$ for vertical saccades). The means for the horizontal and vertical saccades (shown by larger arrows) were not statistically different ($F(2, 21) = 0.03$, $p = 0.98$, $\eta^2 = 0.002$, Bayes Factor (BF_{10}) = 0.032), pointing to no difference between the two at the only significant frequency of 9.4 Hz. This is also brought out in Fig. 2e. Here we fitted subsets of the data with the best-fitting 9.4 Hz sine-wave (of fixed phase) to analyze (post-hoc) separately the peaks and troughs for the two saccadic directions. A two-way ANOVA revealed that while the effect of amplitude (difference between peak and trough) was significant ($F(1, 11) = 6.64$, $p = 0.026$, $\eta_p^2 = 0.38$, 95% CI for amplitude mean difference: [0.17, 2.10]), there was no significant effect of saccadic direction ($F(1, 11) = 0.005$, $p = 0.83$, $\eta_p^2 = 0.005$, 95% CI for saccadic direction mean difference: [-1.04, 0.84]), nor any interaction between saccadic direction and amplitude ($F(1, 11) = 0.024$, $p = 0.88$, $\eta_p^2 = 0.002$, 95% CI for interaction mean difference: [-1.35, 1.56]). Note also that there was a strong average effect of the inducer, $1.71 \pm 0.27^\circ$ for horizontal saccades and $1.40 \pm 0.29^\circ$ for vertical saccades. This reflects the attraction towards the inducer (serial dependence) mentioned earlier, shown here to be equal for horizontal and vertical saccades.

Figure 2f shows the post-hoc variation of peaks and troughs of the best-fitted sinusoidal wave as a function of the orientation of the test stimulus averaged across subjects. It is apparent that the difference in peaks and

Fig. 3 | Oscillations in bias towards 1-back test stimulus. **a** Illustration of how responses were scored, positive if towards the 1-back stimulus. **b** The black line shows the time course of the bias of aggregate data, smoothed over 530 trials (for display purposes only). The gray area around the line represents ± 1 SE computed by bootstrap resampling (1000 reiterations). The colored curve depicts a 9.9 Hz corresponding to the peak spectral amplitude of the combined horizontal and vertical data. **c** GML spectral analysis of the aggregate data, where each trial bias contributed at the exact delay from the saccadic onset. The amplitude spectrum shows a clear peak around 9.9 Hz. The gray region shows the 95% confidence limits of the permutation analysis of the bias, keeping trial saccadic onset delay unaltered. ** indicates FDR corrected $p < 0.05$ in the range 5–25 Hz. **d** 2D vectors of the peak sinusoidal wave at 9.9 Hz for each individual participant for horizontal (blue dots) and vertical (yellow dots) saccades. The blue and yellow arrows show the mean vector of horizontal and vertical saccades, respectively. The length and direction of the arrows indicate the amplitude and phase (relative to time of saccadic onset). **e** The average bias from trials within a 25-ms time window around the peaks and troughs of the 9.9 Hz sinusoidal wave for horizontal and vertical saccades. **f** The average bias from trials within a 25-ms time window around the peaks and troughs of the 9.9 Hz sinusoid for each test orientation. In (e, f), the horizontal line within each violin represents the mean bias, and individual data points are overlaid as dots.



troughs (amplitude) is fairly constant with orientation angle. Neither orientation ($F(5, 115) = 0.69, p = 0.63, \eta_p^2 = 0.03$, 95% CI for orientation mean difference: $[-2.08, 1.61]$) nor the interaction with amplitude ($F(5, 115) = 0.75, p = 0.59, \eta_p^2 = 0.03$, 95% CI for interaction mean difference: $[-2.32, 2.08]$) were significant, while the main effect of amplitude remained highly significant ($F(1, 23) = 10.50, p = 0.004, \eta_p^2 = 0.31$, 95% CI for amplitude mean difference: $[0.45, 2.03]$).

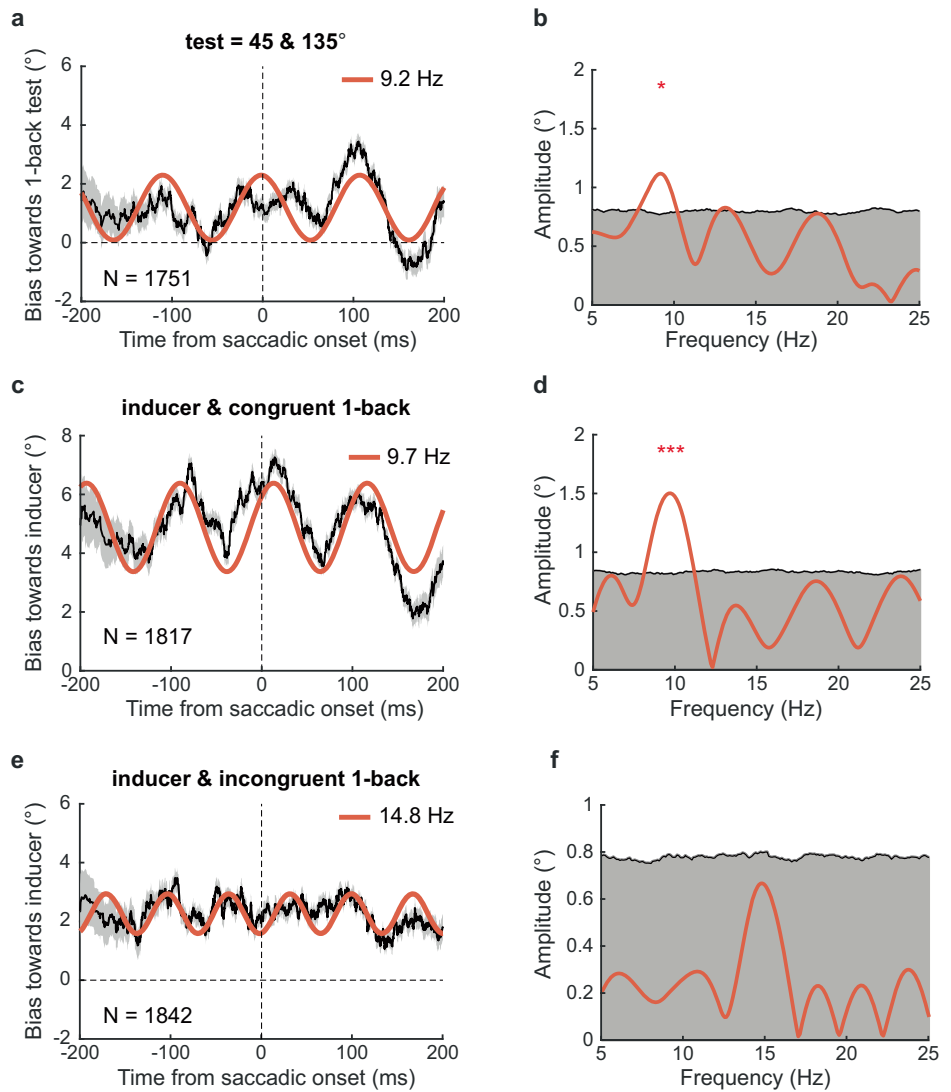
Effect of preceding (1-back) stimuli

The experiment had been designed so every trial was preceded by an inducer ($\pm 15^\circ$ away from the test) to yield maximum serial dependence, with orthogonal inducers as a control. However, there was no strong motivation to attend closely to the inducer, although participants were asked to report which quadrant it was in on about 10% of trials. Another common way to study serial dependence is to consider the effects of the preceding (1-back) test stimuli, which were attended to as the participants were required to judge their orientation. As serial dependence for orientation works over a limited range of difference in orientation and not all combinations of stimuli will be useful. 1-back stimuli with orientations falling in a different quadrant (more than 75° away, half of the trials) should have little or no effect, and were therefore discarded from the computation of the serial dependence. Of the remaining half, one-third were unusable given that 1-back and current stimuli had the same orientation, leaving a total of one-third of all tested trials (5370 trials). These were scored positive if the bias was towards the 1-back stimulus, and negative if away, as illustrated in Fig. 3a.

Again, there was a strong average bias towards the 1-back test ($2.37 \pm 0.45^\circ, t(11) = 5.29, p < 0.001$, Cohen’s $d = 1.53$, 95% CI $[1.38, 3.35]$ for horizontal saccades, and $3.39 \pm 0.33^\circ, t(11) = 10.36, p < 0.001$, Cohen’s $d = 2.99$, 95% CI $[2.67, 4.11]$ for vertical saccades). And again, like the bias towards the inducer, the bias towards the 1-back stimulus was modulated with a strong perceptual oscillation around 9 Hz, of similar amplitude to that towards the inducer (Fig. 3b). The GLM spectral analysis on single trials shows a single clear significant peak at 9.9 Hz (FDR corrected $p = 0.033$, Fig. 3c), plotted with the red curve in Fig. 3b. There was no evidence of other significant frequencies.

Figure 3d shows the amplitudes and phases of a 9.9 Hz modulation (peak frequency for the aggregate data) for all participants. The phase clustering at 9.9 Hz is significant ($42.3^\circ \pm 30.3^\circ$; Hotelling’s T^2 test, $F(2, 22) = 6.93, p = 0.005, \eta^2 = 0.39$; abscissa mean = 0.31 , 95% CIs $[-0.07, 0.92]$; ordinate mean = 0.55 , 95% CIs $[0.18, 0.92]$). Although the average phases of the two saccade directions are slightly different, they are both concentrated in the first quadrant ($7.8^\circ \pm 25.6^\circ$ for horizontal saccades, $65.9^\circ \pm 21.2^\circ$ for vertical saccades, and no evidence of a difference between them: $F(2, 22) = 2.38, p = 0.12, \eta^2 = 0.18, BF_{10} = 0.44$). As in the previous figure, we also looked separately at the post-hoc effects of saccadic direction (Fig. 3e) and test orientation (Fig. 3f) across subjects. Amplitude of modulation in Fig. 3e at 9.9 Hz was highly significant ($F(1, 11) = 11.95, p = 0.005, \eta_p^2 = 0.52$, 95% CI for amplitude mean difference: $[0.46, 2.07]$). Saccadic direction also had a small effect on bias, with average serial dependence slightly stronger for vertical than horizontal saccades ($3.39 \pm 0.33^\circ$

Fig. 4 | Oscillations in bias towards both inducer and 1-back stimuli. **a, c, e** The black line shows the time course of the bias towards 1-back stimuli (and inducers in **c, e**) of aggregate data (only test stimulus is 45 or 135° in **a**), smoothed over 180 trials. The gray area around the line represents ± 1 SE computed by bootstrap resampling (1000 reiterations). The colored curve depicts a 9.2 Hz **(a)**, 9.7 Hz **(c)**, or 14.8 Hz **(e)** corresponding to the peak spectral amplitude of the combined horizontal and vertical data. **b, d, f** GML spectral analysis of the aggregate data, where each trial bias contributed at the exact delay from the saccadic onset. The amplitude spectrum shows a clear peak around 9.2 Hz **(b)**, 9.7 Hz **(d)**, 14.8 Hz **(f)**. The gray region shows the 95% confidence limits of the permutation analysis of the bias, keeping trial saccadic onset delay unaltered. * indicates FDR corrected $p < 0.1$. *** indicates FDR corrected $p < 0.005$.



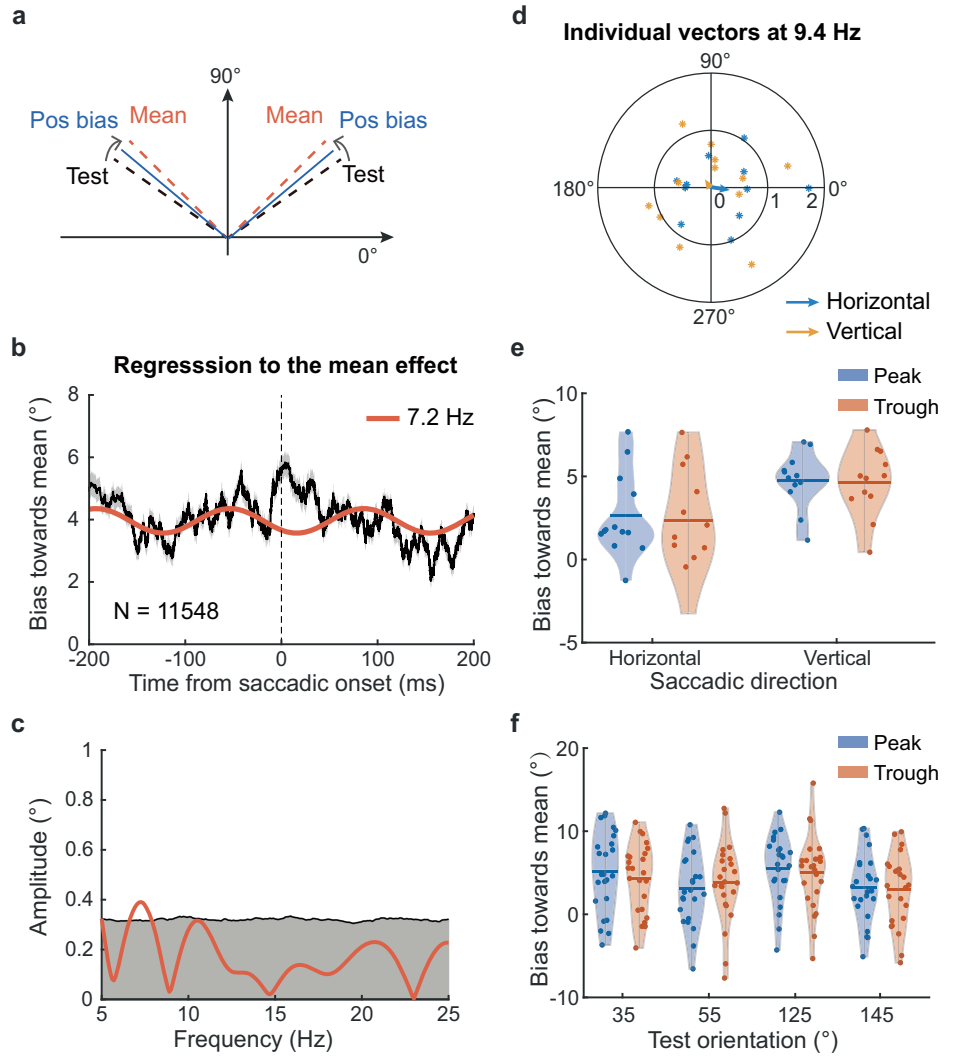
compared with $2.36 \pm 0.45^\circ$; $F(1, 11) = 7.41, p = 0.020, \eta_p^2 = 0.40$, 95% CI for saccadic direction mean difference: $[-2.62, -0.28]$). However, there was no evidence for an interaction between amplitude and saccadic direction ($F(1, 11) = 0.12, p = 0.73, \eta_p^2 = 0.01$, 95% CI for interaction mean difference: $[-1.14, 1.58]$). Figure 3f plots the peaks and troughs as a function of the orientation of the test stimulus across subjects. Again, it is fairly apparent that the amplitude of modulation, given by the difference in peaks and troughs, is highly significant ($F(1, 23) = 15.41, p < 0.001, \eta_p^2 = 0.40$, 95% CI for amplitude mean difference: $[0.59, 1.91]$). There was no significant interaction between orientation and amplitude ($F(5, 115) = 0.59, p = 0.71, \eta_p^2 = 0.03$, 95% CI for amplitude mean difference: $[-2.85, 3.47]$).

However, in this case, there was a significant main effect of orientation ($F(5, 115) = 8.56, p < 0.001, \eta_p^2 = 0.27$, 95% CI for orientation mean difference: $[-2.88, 4.42]$), apparent on inspection. The mean error at 45 and 135° was about 1°, while those for the other four orientations were around 5° ($5.79 \pm 0.54^\circ$ for bias around peaks and $4.70 \pm 0.59^\circ$ for bias around troughs). This is easily explained by another attractive phenomenon, called “regression to the mean” (mentioned earlier), where the mean can be considered as a *prior*^{14,15}. In our experiment, the stimuli clustered around two perceptually very distinct means (at 45 and 135°), so we may expect regression to be towards them. The only stimuli not potentially subject to the central tendency effect were those at the two means, 45 and 135°. However, the other four orientations could regress towards the mean, which

necessarily confounds with attraction towards the 1-back stimulus. For example, a test stimulus at 35° will be attracted to the mean of 45°, and in this analysis the attraction will be scored as attraction towards 1-back (which could only be 45 or 55°). Similarly, a stimulus at 55° will be attracted to the mean of 45°, consistent with attraction to 1-back stimuli of 35 and 45° (the same argument holds for the other quadrant). This is a clear confound (often present in serial dependence studies^{11,53–55}). However, as the oscillations in the bias towards 1-back test remain strong when considering only test stimuli at the mean 45 and 135° (even with only 1751 trials), the confound cannot be the generator of the oscillations.

As both the inducer and the 1-back stimulus bias responses towards them, and both cause alpha oscillations in similar phases, it is reasonable to ask what happens when both occur together, when the 1-back and inducer stimuli are such that both have the same directional slant from the current test stimulus (both clockwise or both counterclockwise). Biases are considered positive if towards both the inducers and 1-back stimuli, negative if away from them. We used both horizontal and vertical saccade data, but the procedure necessarily reduces the number of trials considerably, to 1817. Nevertheless, the oscillations, shown in Fig. 4c, d, are strong and significant (FDR corrected $p < 0.001$), with higher amplitude than either factor considered on its own. The amplitude of the modulations was $1.50 \pm 0.33^\circ$, compared with $0.53 \pm 0.14^\circ$ to the inducer and $0.69 \pm 0.19^\circ$ to the 1-back stimuli alone. The two types of prediction clearly operate together, summing their effects.

Fig. 5 | Oscillations in bias towards the mean orientation. **a** Illustration of how responses were scored, positive if towards the mean orientation in each quadrant. **b** The black line shows the time course of the bias towards mean orientation of aggregate data, smoothed over 400 trials. The gray area around the line represents ± 1 SE computed by bootstrap resampling (1000 reiterations). The colored curve depicts a 7.2 Hz corresponding to the peak spectral amplitude of the combined horizontal and vertical data. **c** GML spectral analysis of the aggregate data, where each trial bias contributed at the exact delay from the saccadic onset. The amplitude spectrum shows a peak around 7.2 Hz. The gray region shows the 95% confidence limits of the permutation analysis of the bias, keeping trial saccadic onset delay unaltered. **d** 2D vectors of the peak sinusoidal wave at 9.4 Hz for each individual participant for horizontal (blue dots) and vertical (yellow dots) saccades. The blue and yellow arrows show the mean vector of horizontal and vertical saccades, respectively. The length and direction of the arrows indicate the amplitude and phase (relative to time of saccadic onset). **e** The average bias from trials within a 25-ms time window around the peaks and troughs of the 9.4 Hz sinusoid for horizontal and vertical saccades. **f** The average bias from trials within a 25-ms time window around the peaks and troughs of the 9.4 Hz sinusoid for each test orientation. In (e, f), the horizontal line within each violin represents the mean bias, and individual data points are overlaid as dots.



We also pitted one effect against the other, considering only trials where the inducer was in the opposite direction from the 1-back stimulus (Fig. 4e, f). Here the two effects canceled each other out, so there was no measurable oscillation at ~9 Hz, and no evidence of any significant oscillation within the entire range. That they cancel completely suggests the oscillations have similar magnitude, despite that the inducer stimulus was temporally closer to the current stimulus.

Effect of central tendency

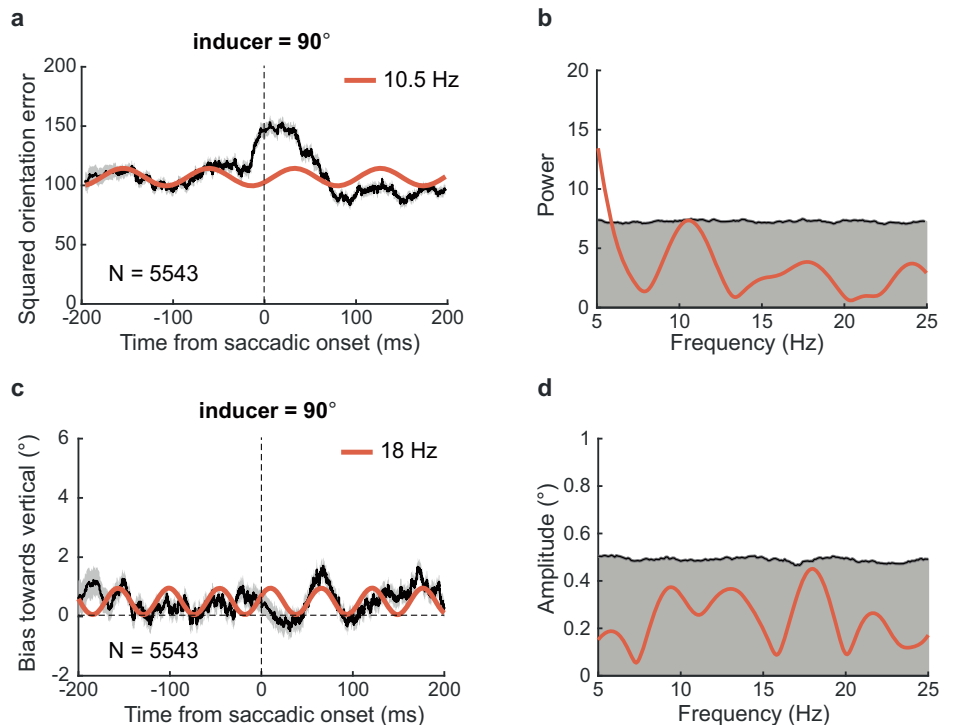
As mentioned above, there exists a third potential source of predictive information: the mean orientation, calculated over a longer time scale than just the previous trial. We therefore examined directly whether *regression to the mean* (or *central tendency*) oscillated over time (as illustrated in Fig. 5a). Figure 5b shows the analysis for all trials (except for test stimuli at mean orientations of 45 or 135°, leaving 11548 trials), coding responses as positive if towards the mean. There is a small but insignificant (FDR corrected $p = 0.42$) oscillation around 7 Hz, but virtually none near 9 Hz (FDR corrected $p = 0.94$ at 9.4 Hz, Fig. 5c). Interestingly, the mean bias was considerable, around 3.5°, and peaked at saccadic onset, agreeing with our previous report. However, the peak in central tendency (red curve in Fig. 5b) near saccadic onset did not correspond to a maximum in the 7.2 Hz oscillation (as with the previous effects for bias towards the inducer or 1-back stimuli), but to a minimum.

We also tested if the 9.4 Hz oscillations generated by other priors (Figs. 2–3) could be revealed from the individual subject data (Fig. 5d–f).

Figure 5d shows the amplitudes and phases of 9.4 Hz modulation (peak frequency for the aggregate data) for all participants. The phase is not clustered ($4.54^\circ \pm 108.67^\circ$, Hotelling’s T^2 test, $F(2, 22) = 0.26$, $p = 0.77$, $\eta^2 = 0.02$; abscissa mean = 0.01, 95% CIs $[-0.06, 0.03]$; ordinate mean = 0.11, 95% CIs $[0.08, 0.20]$). The peak-trough at 9.4 Hz (Fig. 5e, f) shows that, while the mean effect was slightly stronger for vertical than for horizontal saccades (5.29° compared with 3.11° , $F(1, 11) = 9.06$, $p = 0.012$, $\eta_p^2 = 0.45$), the amplitude (difference between peak and trough) of 9.4 Hz modulation did not reach significance under any condition ($F(1, 11) = 0.77$, $p = 0.40$, $\eta_p^2 = 0.07$, 95% CI $[-0.38, 0.89]$ for saccadic direction and $F(1, 23) = 0.96$, $p = 0.33$, $\eta_p^2 = 0.04$ for test orientation, 95% CI $[-0.29, 0.80]$). No interaction effects were found. Pooling all data, without considering saccade direction or test orientation, the difference between peak and trough was clearly non-significant ($t(23) = 0.95$, $p = 0.35$, Cohen’s $d = 0.19$, 95% CI $[-0.30, 0.81]$), with Bayes Factor (BF_{10}) equal to 0.31, conventionally considered substantial evidence in favor of the null effect, indicating that there was no 9.4 Hz modulation.

Thus, while priors from the immediate past – both those associated with inducers and with 1-back stimuli—produced strong alpha oscillations and a weak mean bias, the mean orientation had the opposite effect: very strong mean bias, with no measurable oscillations (for frequencies greater than 5 Hz). This would appear to be a major difference between the action of dynamic priors—which change from trial to trial—and long-term priors derived by averaging over many trials.

Fig. 6 | Orientation errors for the stimuli with orthogonal inducers. The black line shows the time course of the squared orientation error (a) or orientation bias towards vertical (c) of aggregate data, smoothed over 400 trials. The gray area around the line represents ± 1 SE computed by bootstrap resampling (1000 reiterations). The colored curve depicts a 10.5 Hz (a) or 18 Hz (c), corresponding to the peak spectral amplitude of the combined horizontal and vertical data. **b, d** GML spectral analysis of the aggregate data, where each trial bias contributed at the exact delay from the saccadic onset. The amplitude spectrum shows a clear peak around 10.5 Hz (b), 18 Hz (d). The gray region shows the 95% confidence limits of the permutation analysis of the bias, keeping trial saccadic onset delay unaltered.



While the results strongly suggest that the saccade-synchronized alpha modulations reflect the activity of recently presented priors, there is another possibility. Both theoretical and empirical work suggests that the magnitude of serial dependence varies with the reliability of the current stimulus, so less reliable stimuli (with higher intrinsic variance) should demonstrate higher serial dependence (see for example eqn 3.6 of Cicchini et al.⁹) So it is conceivable that it is not the serial dependence per se that oscillates, but the reliability of the current stimulus, affecting its susceptibility to serial dependence in a periodic manner.

We tested this idea by examining how the variance of responses changed over time. Figure 6a plots the squared residuals as a function of time from saccadic onset, considering only trials with orthogonal inducers that are immune to serial dependence bias. Variance is high around saccadic onset, consistent with the low reliability at that time, but there is no systematic oscillation within the alpha range (Fig. 6b, $p = 0.68$ at 10.5 Hz), which could have driven the oscillations observed in Figs. 2 and 3. There may be a significant peak at 5 Hz, which would be consistent with the often-observed theta oscillation in sensitivity^{56–58}, but we are reluctant to give too much weight to this. The period being analyzed was only 400 ms, not sufficient for reliable measurement at 5 Hz (only two periods). The power at 5 Hz could easily be driven by the non-periodic peak at saccadic onset rather than reflect a true periodic oscillation⁵⁹. In any event, this is not relevant to the issues being addressed by this paper.

Figure 6c plots the unsigned error as a function of time relative to saccadic onset, again for the trials with orthogonal inducers, to test for any systematic oscillation of bias (towards the vertical). Again, no evidence of significant oscillations occurred within the alpha range ($p = 0.08$ at 18 Hz, Fig. 6d).

Discussion

The main clear result of this study is that when making orientation judgments at the time of saccades, the biases towards previous stimuli are accompanied by very strong perceptual oscillations in the alpha range (~9 Hz), synchronized to the onset of the saccade. The amplitude of the oscillations could be as high as 1°, of similar magnitude to the average effect. The oscillations could not be explained by oscillations in stimulus reliability,

or in bias towards cardinal axes. The oscillations towards recently displayed stimuli contrasted strongly with the central tendency bias. As previously reported, this bias was far larger than the attraction towards previous stimuli (around 4°), but there were no consistent oscillations in the alpha range associated with the effect.

It is now well accepted that current perception is affected by *priors*, constructed from both immediate and remote perceptual history¹⁶. Much emphasis has been given to the role of recent priors, with paradigms such as *serial dependence*^{4,5}. However, there is also strong evidence for longer-term priors, such as the mean of the distribution, calculated over a longer duration^{13–15}. Central tendency and serial dependence can lead to similar effects, and can be easily confused. For example, as the average of all 1-back responses tends towards the mean, the two can be very hard to distinguish when averaged over many trials. However, the two are very different: serial dependence is based on a dynamic prior that varies on a trial-by-trial basis, whereas central tendency is a more static prior, averaged over a long time course³. Central tendency effects can be present even on the first trial, based, for example, on the layout of the response space of a “number line”¹⁴. Despite their apparent similarities, the two effects can be dissociated⁶⁰, controlled for⁶¹, or separated in modeling⁶².

The current study reports a further, and important distinction between the two types of priors: short-term, dynamic priors (operating over a time period of tens of seconds, as suggested by the “continuity field”³) are associated with alpha rhythms, while long-term priors are not. This distinction is consistent with much previous work. For example, VanRullen and McDonald³⁶ have suggested that visual stimulation leaves a “perceptual echo”, a reverberation at 10 Hz that persists in perceptual memory for over a second. Much evidence has associated this perceptual echo with communication of perceptual history^{29–31}.

Modulation of priors at alpha frequency is also consistent with recent evidence showing that working memory is associated with neural oscillations³⁷ in theta, alpha, beta, and gamma. In particular, alpha-band activity has been observed during working memory tasks, such as the Sternberg task³⁴, and alpha oscillations have been measured in several sensory modalities during working memory maintenance^{40,63}. However, despite strong evidence for the involvement of alpha-band oscillations in

working memory maintenance, the functional interpretation is conflicting. While some studies have related activity in the alpha band to the inhibition of task-irrelevant brain areas^{34,64–66}, others have linked it directly to processes underlying working memory maintenance^{63,67,68}, and a tagging phase mechanism to retrieve the order of events in a temporal sequence⁴¹. But while there is still discussion on the exact role of alpha-band oscillations in working memory, it is clear that they are heavily involved, and may reflect similar mechanisms to those subserving serial dependence.

Alpha rhythms have also been strongly implicated in serial dependence of auditory information³². In an ear-of-origin judgment, alpha oscillations (~9 Hz) occur when the previous stimulus is displayed to the same ear as the current one (but otherwise not). We have also shown, by both psychophysical³³ and EEG techniques⁶⁹, the beta frequency (14–17 Hz) oscillations in face-gender perception related to serial dependence. It is not clear why the oscillations should be at a higher frequency, but presumably, they reflect resonance of different, faster circuits. Nonetheless, the principle seems to be the same: oscillations and serial dependence go hand in hand.

This is not true, however, for regression to the mean. As noted by Hollingworth¹³, all psychophysical judgments tend to show a central tendency. In our experiment, the orientations to be judged were organized in two groups (35, 45, and 55°; and 125, 135, and 145°), each group with its own local mean (45° or 135°). Previous work has shown that observers can keep track of up to four separate means⁷⁰, so it is not unreasonable that their judgments regressed to two separate means. The regression to the mean in orientation judgments is consistent with other effects, such as orientation repulsion bias, the tendency to bias judgments away from the cardinal vertical and horizontal axes towards the oblique. However, this too can be considered as a form of prior, well described in Bayesian terms^{71–73}, so it does not change the substance of the argument. Importantly, these strong biases towards the two separate means (about 4°, compared with 1° bias towards the inducer), were not accompanied by alpha oscillations, or any other consistent oscillation. This was true considering all judgments, or separately those towards their separate means. It is possible that the strong constant bias somehow dampens any potential oscillations (with a floor or ceiling effect), but this seems unlikely, as we were not able to measure any oscillation at all. Thus it would seem that oscillations are not a universal signature of the action of perceptual priors, but are intrinsic only to the short-term, dynamic priors generated by the immediate past. This is very consistent with the recent oscillation-based theories of working memory^{34,35,37,38}.

It is interesting that the oscillations towards the 1-back and inducer stimuli summed together seemingly linearly; and that they subtracted, again linearly, canceling each other out. This suggests that the magnitude of the two effects was similar, despite the differences in the two classes of stimuli. The inducer was temporally closer to the current stimulus (making it potentially stronger^{54,74–77}), but there were less attentional demands on it: participants merely reported its approximate orientation on 10% of the trials, while they had reproduced the orientation of the 1-back stimuli. This is interesting, as evidence from studies showing that reported (and thus memorized, task-relevant, as the 1-back here) stimuli often produce stronger serial dependence effects⁴.

That the modulations caused by the two recent priors interacted quasi-linearly suggests that the two types of serial dependence involve similar mechanisms, potentially indicating shared neural mechanisms, which integrate past information with current sensory inputs. The linear summation of these oscillations implies that the brain might use a unified framework for processing and retaining short-term memory signals, regardless of their specific origin. Moreover, it is also interesting that the effect of horizontal and vertical saccades was similar, with no obvious difference in amplitude or phase of oscillations. This uniformity across saccade directions suggests that the underlying oscillatory mechanisms are robust and generalizable, functioning consistently regardless of the direction of eye movement. This is particularly important given that the direction of the saccade could in principle bias other perceptual phenomenon, acting like *priors*. This could indicate that the integration of pre-saccadic information

to maintain perceptual stability is a fundamental process, not dependent on the specific trajectory of the saccade.

An important aspect of the oscillations is that they are synchronized to saccadic onset. Obviously, if we did not align our data to the saccade, there would be no significant oscillations. The oscillations precede and follow the saccade synchronization. Indeed, the strong bias at saccadic onset is embedded within the saccade-synched oscillations. With the current paradigm it was possible to detect oscillations only 200 ms before saccade onset, but other paradigms have shown that the oscillations precede saccadic onset by at least 1 s^{45,46,49}. While we presume that the oscillation reflects a short-term memory signal of the previous trial or the inducer, it is not obvious how this oscillatory memory is synchronized to the saccade: does the saccade in some way reset the phase of the endogenous oscillation, as suggested by Wutz et al.⁴⁹ and Benedetto et al.⁴²—or is saccadic onset somehow gated by the oscillatory memory signal^{34,36}? The purpose of this synchronization could be to align the neural processes involved in integrating past and current sensory information, thereby enhancing perceptual stability^{1,27,49}. This alignment might help maintain a continuous and stable perception despite the frequent disruptions caused by saccadic eye movements. Alternatively, the gating of saccadic onset by the oscillatory memory signal might serve to optimize the timing of eye movements to coincide with phases of heightened perceptual sensitivity. Although oscillation in peri-saccadic sensitivity are at much lower frequencies, making the understanding of synchronized bias even more difficult. Generally, sensitivity and bias oscillate at different frequencies^{32,46,56,78}, strengthening the idea that the two not only convey independent information, but also the circuits and the feedback are independent at least for the higher cortical representation. Further research is needed to elucidate the mechanisms underlying this synchronization and to understand its functional significance.

Limitations

In this study, the saccades were always of a fixed length and, within a session, of a fixed direction, triggered by a go signal. This could lead to overlearning of the response, and sometimes anticipation. It would be interesting to see if the results extend to more natural viewing conditions, where participants make spontaneous saccades of arbitrary length and direction.

Conclusions

This study underscores the crucial role of alpha oscillations in integrating pre-saccadic prior information with current sensory signals during saccades. We found that orientation judgments were strongly biased towards previous stimuli, with oscillations at ~9 Hz synchronized to saccade onset. The rhythm of the bias was similar for both horizontal and vertical saccades. In contrast, the central tendency bias, while much larger, did not oscillate. These findings suggest that alpha rhythms are essential for communicating short-term perceptual memory across saccades, helping maintain perceptual stability, while long-term priors are communicated differently. Understanding these mechanisms offers insights into how the brain preserves continuity in a dynamic visual world.

Data availability

All single trials data that support our findings are publicly available at the Open Science Framework (<https://osf.io/ev4c9/>).

Code availability

All code for the GLM analyses used to generate the figures are publicly available at the Open Science Framework (<https://osf.io/ev4c9/>).

Received: 11 September 2024; Accepted: 4 March 2025;

Published online: 17 March 2025

References

- Burr, D. C. & Morrone, M. C. Constructing stable spatial maps of the word. *Perception* **41**, 1355–1372 (2012).

2. Ross, J., Morrone, M. C., Goldberg, M. E. & Burr, D. C. Changes in visual perception at the time of saccades. *Trends Neurosci.* **24**, 113–121 (2001).
3. Manassi, M. & Whitney, D. Continuity fields enhance visual perception through positive serial dependence. *Nat. Rev. Psychol.* **3**, 352–366 (2024).
4. Fischer, J. & Whitney, D. Serial dependence in visual perception. *Nat. Neurosci.* **17**, 738–743 (2014).
5. Cicchini, G. M., Anobile, G. & Burr, D. C. Compressive mapping of number to space reflects dynamic encoding mechanisms, not static logarithmic transform. *Proc. Natl. Acad. Sci. USA* **111**, 7867–7872 (2014).
6. Cicchini, G. M., Mikellidou, K. & Burr, D. C. Serial dependence in perception. *Annu. Rev. Psychol.* **75**, 129–154 (2024).
7. Pascucci, D. et al. Serial dependence in visual perception: a review. *J. Vis.* **23**, 9–9 (2023).
8. Manassi, M., Murai, Y. & Whitney, D. Serial dependence in visual perception: a meta-analysis and review. *J. Vis.* **23**, 18 (2023).
9. Cicchini, G. M., Mikellidou, K. & Burr, D. C. The functional role of serial dependence. *Proc. Biol. Sci.* **285**, 20181722 (2018).
10. Ceylan, G., Herzog, M. H. & Pascucci, D. Serial dependence does not originate from low-level visual processing. *Cognition* **212**, 104709 (2021).
11. Gallagher, G. K. & Benton, C. P. Stimulus uncertainty predicts serial dependence in orientation judgements. *J. Vis.* **22**, 6 (2022).
12. You, F. H., Gong, X. M. & Sun, Q. Serial dependencies between form orientation and motion direction are asymmetric. *Front. Psychol.* **14**, 1248307 (2023).
13. Hollingworth, H. L. The central tendency of judgment. *J. Philos. Psychol. Sci. Methods* **7**, 461–469 (1910).
14. Cicchini, G. M., Anobile, G., Chelli, E., Arrighi, R. & Burr, D. C. Uncertainty and prior assumptions, rather than innate logarithmic encoding, explain nonlinear number-to-space mapping. *Psychol. Sci.* **33**, 121–134 (2022).
15. Jazayeri, M. & Shadlen, M. N. Temporal context calibrates interval timing. *Nat. Neurosci.* **13**, 1020–1026 (2010).
16. Chopin, A. & Mamassian, P. Predictive properties of visual adaptation. *Curr. Biol.* **22**, 622–626 (2012).
17. Taubert, J., Alais, D. & Burr, D. Different coding strategies for the perception of stable and changeable facial attributes. *Sci. Rep.* **6**, 1–7 (2016).
18. Diamond, M. R., Ross, J. & Morrone, M. C. Extraretinal control of saccadic suppression. *J. Neurosci.* **20**, 3449–3455 (2000).
19. Burr, D. C., Morrone, M. C. & Ross, J. Selective suppression of the magnocellular visual pathway during saccadic eye movements. *Nature* **371**, 511–513 (1994).
20. Burr, D., Holt, J., Johnstone, J. & Ross, J. Selective depression of motion sensitivity during saccades. *J. Physiol.* **333**, 1–15 (1982).
21. Ross, J., Morrone, M. C. & Burr, D. C. Compression of visual space before saccades. *Nature* **386**, 598–601 (1997).
22. Duhamel, J.-R., Colby, C. L. & Goldberg, M. E. The updating of the representation of visual space in parietal cortex by intended eye movements. *Science* **255**, 90–92 (1992).
23. Wurtz, R. H. Neuronal mechanisms of visual stability. *Vis. Res.* **48**, 2070–2089 (2008).
24. Binda, P. & Morrone, M. C. Vision during saccadic eye movements. *Annu. Rev. Vis. Sci.* **4**, 193–213 (2018).
25. Niemeier, M., Crawford, J. D. & Tweed, D. B. Optimal transsaccadic integration explains distorted spatial perception. *Nature* **422**, 76–80 (2003).
26. Binda, P., Bruno, A., Burr, D. C. & Morrone, M. C. Fusion of visual and auditory stimuli during saccades: a Bayesian explanation for perisaccadic distortions. *J. Neurosci.* **27**, 8525–8532 (2007).
27. Cicchini, G. M., Binda, P., Burr, D. C. & Morrone, M. C. Transient spatiotopic integration across saccadic eye movements mediates visual stability. *J. Neurophysiol.* **109**, 1117–1125 (2013).
28. Xie, X.-Y., Morrone, M. C. & Burr, D. C. Serial dependence in orientation judgments at the time of saccades. *J. Vis.* **23**, 7–7 (2023).
29. Friston, K. J. Waves of prediction. *PLoS Biol.* **17**, e3000426 (2019).
30. Friston, K. J., Bastos, A. M., Pinotsis, D. & Litvak, V. LFP and oscillations—what do they tell us? *Curr. Opin. Neurobiol.* **31**, 1–6 (2015).
31. Alamia, A. & VanRullen, R. Alpha oscillations and traveling waves: signatures of predictive coding? *PLoS Biol.* **17**, e3000487 (2019).
32. Ho, H. T., Burr, D. C., Alais, D. & Morrone, M. C. Auditory perceptual history is propagated through alpha oscillations. *Curr. Biol.* **29**, 4208–4217.e4203 (2019).
33. Bell, J., Burr, D. C., Crookes, K. & Morrone, M. C. Perceptual oscillations in gender classification of faces, contingent on stimulus history. *iScience* **23**, 101573 (2020).
34. Jensen, O., Gelfand, J., Kounios, J. & Lisman, J. E. Oscillations in the alpha band (9–12 Hz) increase with memory load during retention in a short-term memory task. *Cereb. Cortex* **12**, 877–882 (2002).
35. Wianda, E. & Ross, B. The roles of alpha oscillation in working memory retention. *Brain Behav.* **9**, e01263 (2019).
36. VanRullen, R. & Macdonald, J. S. Perceptual echoes at 10 Hz in the human brain. *Curr. Biol.* **22**, 995–999 (2012).
37. Roux, F. & Uhlhaas, P. J. Working memory and neural oscillations: alpha-gamma versus theta-gamma codes for distinct WM information? *Trends Cogn. Sci.* **18**, 16–25 (2014).
38. Klimesch, W., Sauseng, P. & Hanslmayr, S. EEG alpha oscillations: the inhibition-timing hypothesis. *Brain Res. Rev.* **53**, 63–88 (2007).
39. Haegens, S., Osipova, D., Oostenveld, R. & Jensen, O. Somatosensory working memory performance in humans depends on both engagement and disengagement of regions in a distributed network. *Hum. Brain Mapp.* **31**, 26–35 (2010).
40. Kaiser, J., Heidegger, T., Wibral, M., Altmann, C. F. & Lutzenberger, W. Alpha synchronization during auditory spatial short-term memory. *Neuroreport* **18**, 1129–1132 (2007).
41. Huang, Y., Chen, L. & Luo, H. Behavioral oscillation in priming: competing perceptual predictions conveyed in alternating theta-band rhythms. *J. Neurosci.* **35**, 2830–2837 (2015).
42. Benedetto, A., Morrone, M. C. & Tomassini, A. The common rhythm of action and perception. *J. Cogn. Neurosci.* **32**, 187–200 (2020).
43. Neupane, S., Guitton, D. & Pack, C. C. Coherent alpha oscillations link current and future receptive fields during saccades. *Proc. Natl. Acad. Sci. USA* **114**, E5979–E5985 (2017).
44. Benedetto, A. & Morrone, M. C. Visual sensitivity and bias oscillate phase-locked to saccadic eye movements. *J. Vis.* **19**, 15–15 (2019).
45. Hogendoorn, H. Voluntary saccadic eye movements ride the attentional rhythm. *J. Cogn. Neurosci.* **28**, 1625–1635 (2016).
46. Benedetto, A. & Morrone, M. C. Saccadic suppression is embedded within extended oscillatory modulation of sensitivity. *J. Neurosci.* **37**, 3661–3670 (2017).
47. Staudigl, T., Hartl, E., Noachtar, S., Doeller, C. F. & Jensen, O. Saccades are phase-locked to alpha oscillations in the occipital and medial temporal lobe during successful memory encoding. *PLoS Biol.* **15**, e2003404 (2017).
48. Drewes, J. & VanRullen, R. This is the rhythm of your eyes: the phase of ongoing electroencephalogram oscillations modulates saccadic reaction time. *J. Neurosci.* **31**, 4698–4708 (2011).
49. Wutz, A., Muschter, E., van Koningsbruggen, M. G., Weisz, N. & Melcher, D. Temporal integration windows in neural processing and perception aligned to saccadic eye movements. *Curr. Biol.* **26**, 1659–1668 (2016).
50. Benedetto, A., Burr, D. C. & Morrone, M. C. Perceptual oscillation of audiovisual time simultaneity. *eNeuro* **5**, ENEURO.0047–18.2018 (2018).
51. Tomassini, A., Ambrogioni, L., Medendorp, W. P. & Maris, E. Theta oscillations locked to intended actions rhythmically modulate perception. *Elife* **6**, e25618 (2017).

52. Tosato, T., Rohenkohl, G., Dowdall, J. R. & Fries, P. Quantifying rhythmicity in perceptual reports. *Neuroimage* **262**, 119561 (2022).
53. Manassi, M., Liberman, A., Kosovicheva, A., Zhang, K. & Whitney, D. Serial dependence in position occurs at the time of perception. *Psychon. Bull. Rev.* **25**, 2245–2253 (2018).
54. Pascucci, D. et al. Laws of concatenated perception: vision goes for novelty, decisions for perseverance. *PLoS Biol.* **17**, e3000144 (2019).
55. van Bergen, R. S. & Jehee, J. F. M. Probabilistic representation in human visual cortex reflects uncertainty in serial decisions. *J. Neurosci.* **39**, 8164–8176 (2019).
56. Benedetto, A., Spinelli, D. & Morrone, M. C. Rhythmic modulation of visual contrast discrimination triggered by action. *Proc. R. Soc. B Biol. Sci.* **283**, 20160692 (2016).
57. Fiebelkorn, I. C., Saalman, Y. B. & Kastner, S. Rhythmic sampling within and between objects despite sustained attention at a cued location. *Curr. Biol.* **23**, 2553–2558 (2013).
58. Landau, A. N. & Fries, P. Attention samples stimuli rhythmically. *Curr. Biol.* **22**, 1000–1004 (2012).
59. Brookshire, G. Putative rhythms in attentional switching can be explained by aperiodic temporal structure. *Nat. Hum. Behav.* **6**, 1280–1291 (2022).
60. Roseboom, W. Serial dependence in timing perception. *J. Exp. Psychol.: Hum. Percept. Perform.* **45**, 100 (2019).
61. Liberman, A., Fischer, J. & Whitney, D. Serial dependence in the perception of faces. *Curr. Biol.* **24**, 2569–2574 (2014).
62. Xia, Y., Leib, A. Y. & Whitney, D. Serial dependence in the perception of attractiveness. *J. Vis.* **16**, 28–28 (2016).
63. Herrmann, C. S., Senkowski, D. & Röttger, S. Phase-locking and amplitude modulations of EEG alpha: Two measures reflect different cognitive processes in a working memory task. *Exp. Psychol.* **51**, 311–318 (2004).
64. Medendorp, W. P. et al. Oscillatory activity in human parietal and occipital cortex shows hemispheric lateralization and memory effects in a delayed double-step saccade task. *Cereb. Cortex* **17**, 2364–2374 (2007).
65. Jokisch, D. & Jensen, O. Modulation of gamma and alpha activity during a working memory task engaging the dorsal or ventral stream. *J. Neurosci.* **27**, 3244–3251 (2007).
66. Sauseng, P. et al. Brain oscillatory substrates of visual short-term memory capacity. *Curr. Biol.* **19**, 1846–1852 (2009).
67. Leiberg, S., Lutzenberger, W. & Kaiser, J. Effects of memory load on cortical oscillatory activity during auditory pattern working memory. *Brain Res.* **1120**, 131–140 (2006).
68. Palva, S., Kulashekhar, S., Hämäläinen, M. & Palva, J. M. Localization of cortical phase and amplitude dynamics during visual working memory encoding and retention. *J. Neurosci.* **31**, 5013–5025 (2011).
69. Ranieri, G., Bell, J., Burr, D. & Morrone, M. C. Serial dependence in face-gender classification revealed in low-beta frequency EEG. *bioRxiv*, 2023.2010.2027.564174 (2023). in press.
70. Morgan, M. J. On the scaling of size judgements by orientational cues. *Vis. Res.* **32**, 1433–1445 (1992).
71. Van Bergen, R. S., Ma, W. J., Pratte, M. S. & Jehee, J. F. Sensory uncertainty decoded from visual cortex predicts behavior. *Nat. Neurosci.* **18**, 1728–1730 (2015).
72. Wei, X.-X. & Stocker, A. A. A Bayesian observer model constrained by efficient coding can explain ‘anti-Bayesian’ percepts. *Nat. Neurosci.* **18**, 1509–1517 (2015).
73. Henderson, M. & Serences, J. T. Biased orientation representations can be explained by experience with nonuniform training set statistics. *J. Vis.* **21**, 10 (2021).
74. Abreo, S., Gergen, A., Gupta, N. & Samaha, J. Effects of satisfying and violating expectations on serial dependence. *J. Vis.* **23**, 6 (2023).
75. Blonde, P., Kristjansson, A. & Pascucci, D. Tuning perception and decisions to temporal context. *iScience* **26**, 108008 (2023).
76. Ceylan, G. & Pascucci, D. Attractive and repulsive serial dependence: the role of task relevance, the passage of time, and the number of stimuli. *J. Vis.* **23**, 8 (2023).
77. Houborg, C., Kristjansson, A., Tanrikulu, O. D. & Pascucci, D. The role of secondary features in serial dependence. *J. Vis.* **23**, 21 (2023).
78. Ho, H. T., Leung, J., Burr, D. C., Alais, D. & Morrone, M. C. Auditory sensitivity and decision criteria oscillate at different frequencies separately for the two ears. *Curr. Biol.* **27**, 3643–3649.e3643 (2017).

Acknowledgements

This research was financed by the European Union (EU) and Horizon 2020—grant agreement No. 832813—ERC Advanced “Spatio-temporal mechanisms of generative perception—GenPercept” and Natural Science Foundation of China Grant 31900799. The funders had no role in study design, data collection and analysis, decision to publish or preparation of the manuscript.

Author contributions

X.X. Conceptualization, Methodology, Data Collection, Data Analysis, Writing and revision; M.C.M., Conceptualization, Methodology, Data Analysis, Writing and revision; D.C.B.; Conceptualization, Methodology, Writing and revision.

Competing interests

The authors declare no competing interests.

Additional information

Supplementary information The online version contains supplementary material available at <https://doi.org/10.1038/s44271-025-00224-7>.

Correspondence and requests for materials should be addressed to Xin-Yu Xie.

Peer review information *Communications Psychology* thanks Camille Fakche and the other, anonymous, reviewer(s) for their contribution to the peer review of this work. Primary Handling Editors: Troby Ka-Yan Lui. A peer review file is available.

Reprints and permissions information is available at <http://www.nature.com/reprints>

Publisher’s note Springer Nature remains neutral with regard to jurisdictional claims in published maps and institutional affiliations.

Open Access This article is licensed under a Creative Commons Attribution-NonCommercial-NoDerivatives 4.0 International License, which permits any non-commercial use, sharing, distribution and reproduction in any medium or format, as long as you give appropriate credit to the original author(s) and the source, provide a link to the Creative Commons licence, and indicate if you modified the licensed material. You do not have permission under this licence to share adapted material derived from this article or parts of it. The images or other third party material in this article are included in the article’s Creative Commons licence, unless indicated otherwise in a credit line to the material. If material is not included in the article’s Creative Commons licence and your intended use is not permitted by statutory regulation or exceeds the permitted use, you will need to obtain permission directly from the copyright holder. To view a copy of this licence, visit <http://creativecommons.org/licenses/by-nc-nd/4.0/>.

© The Author(s) 2025